Frictional Coupling between Sliding and Spinning Motion

Zénó Farkas,[1] Guido Bartels,[1] Tamás Unger,[2] and Dietrich E. Wolf[1]

[1]*Institute of Physics, University Duisburg-Essen, D-47048 Duisburg, Germany*

[2]*Department of Theoretical Physics, Budapest University of Technology and Economics, H-1111 Budapest, Hungary*

(Received 27 September 2002; published 18 June 2003)

The tangential motion at the contact of two solid objects is studied. It consists of a sliding and a spinning degree of freedom (no rolling). We show that the friction force and torque are inherently coupled. As a simple test system, a sliding and spinning disk on a horizontal flat surface is considered. We calculate, and also measure, how the disk slows down and find that it always stops its sliding and spinning motion at the same moment. We discuss the impact of this coupling between friction force and torque on the physics of granular materials.

DOI: 10.1103/PhysRevLett.90.248302 PACS numbers: 81.05.Rm, 45.70.–n, 46.55.+d, 81.40.Pq

Imagine two identical disks sliding with the same initial velocity on a table. The only difference is that one of them is also spinning. What do you expect: (a) The two disks slide the same distance until they stop, (b) the spinning disk slides further, or (c) the non-spinning disk slides further? The correct answer is that the spinning disk slides further, because the spinning motion reduces the sliding friction force. Furthermore, the sliding and spinning motion stop at the same moment, no matter what the initial condition is. This phenomenon is evaluated quantitatively in this Letter.

The results are important in more general contexts: As a first example we consider the porosity of a dry powder of faceted particles. If it simply settles under its own weight or is pushed together by means of a piston, the porosity depends on the friction coefficient [1]. Further compaction requires the collective rearrangement of particles due to, e.g., tapping [2,3]. During the settling of a porous powder, some contacts between grains will in general be subject to a torque component normal to the contact area. Therefore, torsion friction should be important, if the powder particles are faceted and hence have large contact areas. For this case we are going to show that one overestimates the porosity of the powder significantly, if one ignores the coupling between torque and sliding friction (in the framework of the Coulomb friction model). Avalanches or chute flow of dry granular material provide a second example. Here again one overestimates dissipation if one does not take the coupling of sliding and spinning motion into account.

At first, however, to explain the coupling between sliding and spinning motion, we consider a flat disk on a horizontal flat surface with nonzero initial translational and angular velocity. The disk is lying on one of its sides, and we assume that this side is in full contact with the table during the motion [see Fig. 1(a)]. The friction force and torque acting on the disk will slow down the sliding and spinning motion until the disk stops moving. We address two questions: (i) How are the friction force and torque related to each other, and (ii) what does this imply for the coupling of sliding and spinning motion?

First we calculate the friction force and torque acting on the disk as a function of its instantaneous velocity and angular velocity. We apply the Coulomb friction law, which states that the magnitude of the friction force is proportional to the normal force, while its direction is opposite to the direction of the surfaces' relative velocity. Assuming that the normal stress is uniform (equal to $F_n/\pi R^2$) throughout the contact area, the friction force is

$$\mathbf{F} = -\frac{\mu F_n}{\pi R^2}\int_{\mathbf{r}\in A}\frac{\mathbf{v}+\boldsymbol{\omega}\times\mathbf{r}}{|\mathbf{v}+\boldsymbol{\omega}\times\mathbf{r}|}\,d^2r, \tag{1}$$

where R is the radius, $\mathbf{v}$ is the velocity, and $\boldsymbol{\omega}$ is the angular velocity of the disk, μ is the friction coefficient, and the integration extends over the area of the disk with $\mathbf{r}$ vectors starting at the center. F_n is the normal component of the force pressing the objects together at the contact; in our case, $F_n = mg$, where m is the mass of the disk and g is the gravitational acceleration. We found it useful to introduce the dimensionless quantity $\varepsilon = v/R\omega$ with $v = |\mathbf{v}|$ and $\omega = |\boldsymbol{\omega}|$, because the friction force depends on v and ω only through this combination:

$$\mathbf{F} = -\frac{\mu F_n}{\pi}\int_{\tilde{\mathbf{r}}\in A_1}\frac{\varepsilon\mathbf{e}_v+\mathbf{e}_\omega\times\tilde{\mathbf{r}}}{|\varepsilon\mathbf{e}_v+\mathbf{e}_\omega\times\tilde{\mathbf{r}}|}\,d^2\tilde{r}, \tag{2}$$

where $\mathbf{e}_v = \mathbf{v}/v$, $\mathbf{e}_\omega = \boldsymbol{\omega}/\omega$, $\tilde{\mathbf{r}} = \mathbf{r}/R$, and A_1 is the area

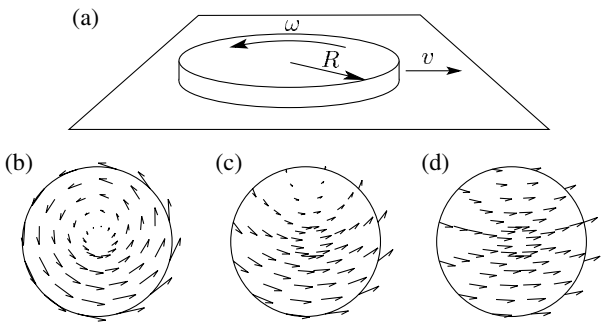

FIG. 1. (a) A sliding and spinning disk on a flat horizontal surface. (b)–(d) The relative velocity field on the surface of the disk at $\varepsilon = 0.2$, $\varepsilon = 1$, and $\varepsilon = 5$, respectively ($\varepsilon = v/R\omega$).

of the unit disk. Figures 1(b)–1(d) show local relative velocities on the surface of the disk for various values of ε. Note that the local friction force does not depend on the absolute value of the relative velocity, only on its direction. After evaluating the integral in Eq. (2) one gets $\mathbf{F} = -\mu F_{\mathrm{n}} \mathcal{F}(\varepsilon)\mathbf{e}_v$, where

$$\mathcal{F}(\varepsilon) = \begin{cases} \frac{4}{3}\frac{(\varepsilon^2+1)E(\varepsilon)+(\varepsilon^2-1)K(\varepsilon)}{\varepsilon\pi}, & \varepsilon \le 1 \\ \frac{4}{3}\frac{(\varepsilon^2+1)E(\frac{1}{\varepsilon})-(\varepsilon^2-1)K(\frac{1}{\varepsilon})}{\pi}, & \varepsilon \ge 1. \end{cases}$$

Here $K(\varepsilon)$ and $E(\varepsilon)$ are the complete elliptic integral functions of the first and the second kind, respectively [4]. The two parts of $\mathcal{F}(\varepsilon)$ are smoothly connected at $\varepsilon = 1$, since $\lim_{\varepsilon\to 1}\mathcal{F}(\varepsilon) = 8/3\pi$ and $\lim_{\varepsilon\to 1}\mathcal{F}'(\varepsilon) = 4/3\pi$ from both the left-hand and the right-hand sides. Here prime denotes differentiation with respect to ε. The limiting values are $\mathcal{F}(0) = 0$ and $\lim_{\varepsilon\to\infty}\mathcal{F}(\varepsilon) = 1$. Note that the sliding trajectory is a straight line, because the friction force is collinear with the velocity. As we show below, this is in general not the case if the normal stress is not uniform throughout the contact area.

The friction torque is

$$\mathbf{T} = -\frac{\mu F_{\mathrm{n}}}{R^2\pi}\int_{\mathbf{r}\in A} \mathbf{r} \times \frac{\mathbf{v}+\boldsymbol{\omega}\times\mathbf{r}}{|\mathbf{v}+\boldsymbol{\omega}\times\mathbf{r}|}\, d^2r, \tag{3}$$

and after calculating the integral we get $\mathbf{T} = -\mu F_{\mathrm{n}} R \mathcal{T}(\varepsilon)\mathbf{e}_\omega$, where

$$\mathcal{T}(\varepsilon) = \begin{cases} \frac{4}{9}\frac{(4-2\varepsilon^2)E(\varepsilon)+(\varepsilon^2-1)K(\varepsilon)}{\pi}, & \varepsilon \le 1 \\ \frac{4}{9}\frac{(4-2\varepsilon^2)E(\frac{1}{\varepsilon})+(2\varepsilon^2-5+\frac{3}{\varepsilon^2})K(\frac{1}{\varepsilon})}{\varepsilon\pi}, & \varepsilon \ge 1. \end{cases}$$

The two parts of this function are also smoothly connected, as $\lim_{\varepsilon\to 1}\mathcal{T}(\varepsilon) = 8/9\pi$ and $\lim_{\varepsilon\to 1}\mathcal{T}'(\varepsilon) = -4/3\pi$ from both the left-hand and the right-hand sides. The limiting values are $\mathcal{T}(0) = 2/3$ and $\lim_{\varepsilon\to\infty}\mathcal{T}(\varepsilon) = 0$. Figure 2 shows $\mathcal{F}(\varepsilon)$ and $\mathcal{T}(\varepsilon)$ and also the $\mathcal{F}(\mathcal{T})$ function. This latter exists and is invertible because both $\mathcal{F}(\varepsilon)$ and $\mathcal{T}(\varepsilon)$ are strictly monotonic functions.

Now let us calculate how a sliding and spinning disk is slowing down. Assuming that only gravity and friction forces are acting, the scalar equations of motion are

$$m\frac{dv}{dt} = -\mu mg\mathcal{F}(\varepsilon), \tag{4}$$

$$I\frac{d\omega}{dt} = -\mu mgR\mathcal{T}(\varepsilon), \tag{5}$$

where the moment of inertia of a cylindrical disk is $I = mR^2/2$. By introducing dimensionless velocities and time as $v^* = v/\sqrt{Rg}\mu$, $\omega^* = \omega\sqrt{R/g}/\mu$, and $t^* = t\sqrt{g/R}$, Eqs. (4) and (5) reduce to

$$\frac{dv^*}{dt^*} = -\mathcal{F}(\varepsilon), \tag{6}$$

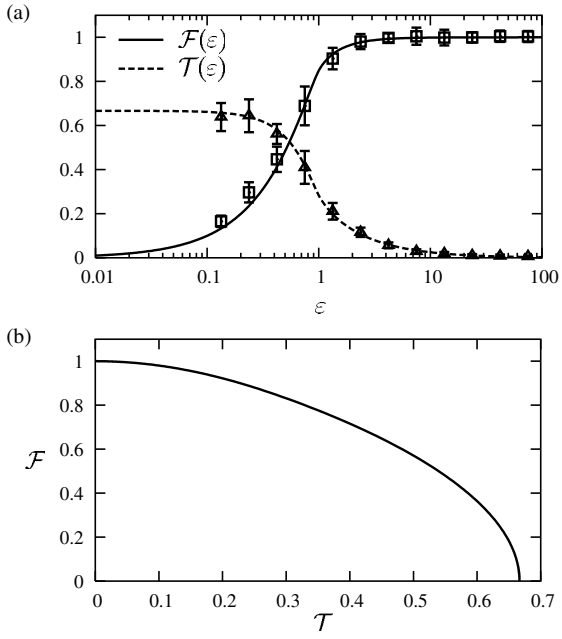

FIG. 2. (a) The dimensionless friction force and torque, $\mathcal{F}$ and $\mathcal{T}$, as functions of the dimensionless velocity parameter ε. Squares and triangles with error bars represent experimental data (explained in the text). (b) The friction force and torque are coupled: the curve shows the possible $(\mathcal{F}, \mathcal{T})$ pairs.

$$\frac{d\omega^*}{dt^*} = -2\mathcal{T}(\varepsilon), \tag{7}$$

with $\varepsilon = v^*/\omega^*$. As $\mathcal{F}(\varepsilon)$ and $\mathcal{T}(\varepsilon)$ are positive for $\varepsilon > 0$, the translational and angular velocities are strictly monotonically decreasing in time, as expected. Now the question arises: Is it possible that any of them reaches zero before the other, i.e., may it happen that an initially sliding and spinning disk after some time is only sliding or spinning? Let us first discuss qualitatively what happens. If the velocity is much higher than the angular velocity ($v \gg R\omega$, i.e., $\varepsilon \gg 1$), then the friction torque is negligible compared to the force; see Fig. 2(a). Therefore, the velocity decreases with a higher rate than the angular velocity, and ε decreases. On the other hand, if the angular velocity is much higher than the velocity ($\varepsilon \ll 1$), then the friction torque is higher than the force, and ε increases. Thus, a negative feedback effectively equilibrates the sliding and spinning motion. Indeed, we now prove that ε always tends to the same value, $\varepsilon_0 \approx 0.653$, when the motion stops. This means that ω^* and v^* approach zero in proportion to each other, which implies that *the disk always stops its sliding and spinning motion at the same moment.*

To prove that ε always has this value at the end of the motion, we derive an autonomous differential equation for ε from Eqs. (6) and (7) using the variable transformation $x = -\ln\omega^*$:

$$\frac{d\varepsilon}{dx} = \varepsilon - \frac{\mathcal{F}(\varepsilon)}{2\mathcal{T}(\varepsilon)} \equiv f(\varepsilon). \tag{8}$$

Note that $\omega^* \to 0$, the condition of stopping, now corresponds to $x \to \infty$ (with the exception of pure sliding motion). For small ε the right-hand side of Eq. (8) vanishes like $f(\varepsilon) \approx \varepsilon/4$, while it behaves asymptotically for $\varepsilon \to \infty$ like $f(\varepsilon) \approx -\varepsilon$. In between, at ε_0, it changes sign (Fig. 3). Therefore, Eq. (8) has three fixed points: Two of them, $\varepsilon = 0$ and $\varepsilon = \infty$, are trivial and correspond to pure spinning or pure sliding motion, respectively. For all other initial conditions ($0 < \varepsilon < \infty$) corresponding to initial sliding *and* spinning, ε_0 is the attractive fixed point, meaning that ε has this value just before the disk stops its motion, which is what we wanted to prove.

To check the prediction that for a spinning disk the Coulomb friction force is velocity dependent, we performed an experiment to measure the friction force and torque acting on a sliding and spinning disk. We set a plastic disk, with 8 cm radius and 2 cm width, into motion manually on a horizontal polyamid fabric surface several times and recorded its motion with a Sony DCR-VX2000E PAL digital video camera (25 images/second). Then we processed the images to obtain the position and the orientation of the disk as functions of time. The upper side of the disk had an appropriately colored pattern, so that the image processing could be performed almost fully automatically. Third-degree polynomials were fitted to the spatial (x and y directions) and angular position of the disk on the first 11 consecutive video frames of each throw, and the derivatives of these polynomials were evaluated at the middle (6th frame) of this window to get the approximate translational and angular velocity and acceleration in that moment. The measured velocities varied between 0.1 and 2.2 m/s, while the angular velocities varied between 0.002 and 37.1 Hz.

Figure 2(a) shows that according to the theory the friction force saturates to its usual, sliding-only value at around $\varepsilon \approx 10$. Hence, using Eq. (4), we were able to fit the value of μg to the acceleration data in the cases where $\varepsilon > 10$ (68 out of 530 data points). The result was $\mu g = 3.60 \pm 0.01$ m/s^2, corresponding to a sliding friction coefficient $\mu = 0.37 \pm 0.01$ ($g = 9.81$ m/s^2). We had altogether 764 data points (throws), but we used only the last 530 data points. The reason was that, considering only the subset of data points for $\varepsilon > 10$, we observed initially some variation of the translational acceleration. We interpret this variation as an indication of wear, which changed the friction coefficient. However, after 200 throws, these variations could no longer be observed, so that μ could be determined reliably from the data as described above. As we had no further parameter to fit, we were able to process the rest of the data to get $\mathcal{F}$ and $\mathcal{T}$ as functions of ε by utilizing Eqs. (4) and (5). Figure 2(a) shows the average of the 530 data points. The error bars were obtained by averaging the data within logarithmic bins of the ε values. Each bin contained data for many different velocities (and corresponding angular velocities). Thus, the experiment confirms that different velocities with the same ε lead to the same force and torque. Moreover, the data shown in Fig. 2(a) are in agreement with the nontrivial prediction of the theory, that the effective sliding friction coefficient is dynamically reduced by spinning motion. The experiment also confirmed that sliding and spinning stopped at the same moment (results not shown here).

We used the sliding and spinning disk as a simple, illustrative example to show how friction force and torque are coupled. In this case we were able to derive all results analytically, because the local pressure is everywhere the same in the contact area. However, in general the pressure distribution over the contact area will be nonuniform. As an example, if we replace the flat disk by a cylinder standing on one of its flat faces, then the friction force leads to a torque with respect to the center of mass. Provided that the cylinder does not topple, this torque must be compensated by a pressure increase at the front and a pressure decrease at the rear part of the contact area (see Fig. 4). Therefore, the spinning motion induces a friction component perpendicular to the translational motion, in the direction of $\mathbf{e}_v \times \mathbf{e}_\omega$. Hence, in contrast to the straight sliding of a flat spinning disk, the path of

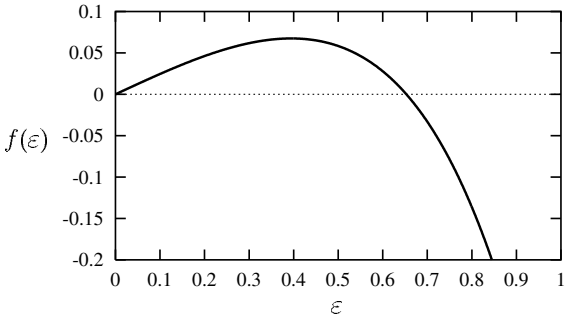

FIG. 3. Function $f(\varepsilon) = \varepsilon - \mathcal{F}(\varepsilon)/2\mathcal{T}(\varepsilon)$, the right-hand side of differential Eq. (8). It has zero value at $\varepsilon = 0$ and $\varepsilon_0 \approx 0.653$ and is positive for $0 < \varepsilon < \varepsilon_0$, negative for $\varepsilon_0 < \varepsilon$.

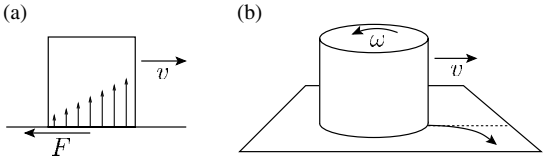

FIG. 4. (a) The pressure distribution of the normal force acting on a sliding tall cylinder is nonuniform, because it has to counterbalance the torque exerted by the friction force F, provided that the cylinder does not topple (schematic side view). (b) As a consequence of the nonuniform normal pressure distribution, if the cylinder is also spinning, the net friction force is not collinear with the velocity; therefore, the trajectory is curved.

the cylinder will be curved in this direction. This resembles the Magnus effect [5], although the physical origin is completely different. To estimate the order of magnitude of this effect for a homogeneous cylinder of height H, we assume a linear pressure correction $\Delta p = \alpha \mathbf{r} \cdot \mathbf{e}_v$, which occurs as a weight in the integrand of Eq. (1). By symmetry this does not change the component $\mathbf{F} \cdot \mathbf{e}_v = -\mu F_n \mathcal{F}(\varepsilon)$. Therefore, α can be estimated by the requirement that the torque $FH/2$ must be compensated so that the cylinder slides without toppling. One obtains $\alpha = 2FH/\pi R^4$. Evaluating Eq. (1) including the additional linear pressure in the integrand gives a force component $\mu^2 F_n \mathcal{F}(\varepsilon)(H/R)\mathcal{F}_M(\varepsilon)$ whose direction is $\mathbf{e}_v \times \mathbf{e}_\omega$. The function $\mathcal{F}_M(\varepsilon)$ is similar to $\mathcal{T}(\varepsilon)$, its special values are $\mathcal{F}_M(0) = 2/3$, $\mathcal{F}_M(1) = 64/45\pi \approx 0.45$, and $\lim_{\varepsilon\to\infty} \mathcal{F}_M(\varepsilon) = 0$. Thus, the force component perpendicular to the velocity is just the parallel component multiplied by the friction coefficient, the aspect ratio H/R of the cylinder, and function $\mathcal{F}_M(\varepsilon)$ [6].

The pressure distribution can also depend on the shape and elastic properties of the sliding body. For instance, if it is a sphere, linear elasticity theory predicts a $\sqrt{1 - r^2/R^2}$ shaped radial pressure function [7]. We calculated the $\mathcal{F}(\varepsilon)$ and $\mathcal{T}(\varepsilon)$ curves numerically for this case and found that their qualitative behavior remains the same [8]. Therefore, coupling between the friction force and torque is still present: For large ε torsion friction is suppressed by sliding; for small ε sliding friction gets reduced by spinning. This may explain why the translational motion of a fast spinning top is hardly decelerated.

Now let us come back to the examples of dry powder settling and of chute flow, which we mentioned in the beginning. Typical sliding velocities will be comparable to ωR_p, so that $\varepsilon \approx R_p/R$, where R_p denotes the particle radius and R the contact radius, as before. Hence, for faceted particles $\varepsilon \approx 1$. As shown in Fig. 2(b), ignoring the coupling (i.e., setting $\mathcal{F} = 1$ and $\mathcal{T} = 2/3$ irrespective of the value of ε) leads to an overestimation of friction force and torque by as much as 30%–50%. This means that the compaction of the powder is actually easier than one would expect. Likewise, the dissipation rate at the particle contacts in an avalanche $\mu F_n v \mathcal{F}(\varepsilon) + \mu F_n R\omega \mathcal{T}(\varepsilon) = \mu F_n v[\mathcal{F}(\varepsilon) + \mathcal{T}(\varepsilon)/\varepsilon]$ is smaller than $\mu F_n v(1 + 2/3\varepsilon)$, which would be the value if one ignored the coupling. (For $\varepsilon \approx 1$ this means a reduction by 30%.) However, for hard spherical particles, $\varepsilon \gg 1$, so that torsion friction should be unimportant in the sliding case, and the friction force is not reduced.

We have preliminary experimental results which show that a qualitatively similar coupling as in Fig. 2(b) exists also in the static case: A torque which is too small to set a disk into rotation still reduces the threshold force needed to induce sliding, and vice versa. This shows that also the static stability of a powder can be strongly overestimated if the coupling is ignored.

In this Letter, we focused on the frictional coupling between tangential velocity and normal angular velocity at a contact. In granular media there is also dissipation connected to the other two modes of relative motion, which are described by a normal velocity (normal restitution mode) and a tangential angular velocity (rolling mode), and the question may be posed whether they are coupled as well. Indeed, there is a clear indication for such a coupling for viscoelastic particles [9–11]; however, the dynamical consequences of such a coupling have not yet been worked out in detail. Moreover, for collisions with high speed, plastic deformation cannot be neglected, and for this case the coupling between normal restitution and rolling mode has not yet been studied. Our discussion of the frictional "Magnus effect" indicates that in general all four modes of relative motion (sliding, spinning, rolling, and normal restitution mode) could be coupled.

We thank János Kertész, Péter Gnädig, Dirk Kadau, and Lothar Brendel for useful discussions and Detlef Wildenberg (Audio-Visual Media Center, Gerhard-Mercator University) for his help with video recording the experiment. We acknowledge funding from DFG Graduate College 277 (G. B.), DFG Grant No. Wo577/3-1 (Z. F.), DAAD (T. U.), OTKA Grant No. T035028 (T. U.), and Federal Mogul Technology GmbH.

[1] D. Kadau, G. Bartels, L. Brendel, and D. E. Wolf, Phase Transitions **76**, 315 (2003).
[2] J. B. Knight, C. G. Fandrich, C. N. Lau, H. M. Jaeger, and S. R. Nagel, Phys. Rev. E **51**, 3957 (1995).
[3] M. Nicodemi, A. Coniglio, and H. J. Herrmann, Phys. Rev. E **55**, 3962 (1997).
[4] M. Abramowitz and I. A. Stegun, *Handbook of Mathematical Functions* (Dover, New York, 1965).
[5] P. M. Gerhart, R. J. Gross, and J. I. Hochstein, *Fundamentals of Fluid Mechanics* (Addison-Wesley, Reading, MA, 1992).
[6] For the disk used in the experiment the aspect ratio was 1/4, and the deviation from a straight trajectory was only very small.
[7] L. D. Landau and E. M. Lifshitz, *Theory of Elasticity* (Pergamon Press, London, 1959).
[8] In the case of a sphere, rolling also should be taken into account, leading to further complications. However, for the sake of simplicity, here we neglected rolling.
[9] N. V. Brilliantov and T. Pöschel, Europhys. Lett. **42**, 511 (1998).
[10] T. Pöschel, T. Schwager, and N. V. Brilliantov, Eur. Phys. J. B **10**, 169 (1999).
[11] R. Ramírez, T. Pöschel, N. V. Brilliantov, and T. Schwager, Phys. Rev. E **60**, 4465 (1999).